Sign-Reversing Orbital Polarization in the Nematic Phase of FeSe due to the C_2 Symmetry Breaking in the Self-Energy

Seiichiro Onari,[1,2] Youichi Yamakawa,[3] and Hiroshi Kontani[3]
[1]Department of Physics, Okayama University, Okayama 700-8530, Japan
[2]Research Institute for Interdisciplinary Science, Okayama University, Okayama 700-8530, Japan
[3]Department of Physics, Nagoya University, Furo-cho, Nagoya 464-8602, Japan
(Received 24 September 2015; revised manuscript received 23 February 2016; published 2 June 2016)

To understand the nematicity in Fe-based superconductors, nontrivial $\boldsymbol{k}$ dependence of the orbital polarization $[\Delta E_{xz}(\boldsymbol{k}), \Delta E_{yz}(\boldsymbol{k})]$ in the nematic phase, such as the sign reversal of the orbital splitting between Γ and X, Y points in FeSe, provides significant information. To solve this problem, we study the spontaneous symmetry breaking with respect to the orbital polarization and spin susceptibility self-consistently. In FeSe, due to the sign-reversing orbital order, the hole and electron pockets are elongated along the k_y and k_x axes, respectively, consistently with experiments. In addition, an electron pocket splits into two Dirac cone Fermi pockets while increasing the orbital polarization. The orbital order in Fe-based superconductors originates from the strong positive feedback between the nematic orbital order and spin susceptibility.

DOI: 10.1103/PhysRevLett.116.227001

The spontaneous symmetry breaking from C_4 to C_2 symmetry, the so called electronic nematic transition, is one of the fundamental unsolved electronic properties in Fe-based superconductors. To explain this nematicity, both the spin-nematic scenario [1–6] and the orbital order scenario [7–13] have been studied intensively. Above the structural transition temperatures $T_{\rm str}$, the large enhancement of the electronic nematic susceptibility predicted by both scenarios [1,10] is actually observed by the measurements of the softening of the shear modulus C_{66} [1,10,14,15], Raman spectroscopy, [16–18], and in-plane resistivity anisotropy $\Delta\rho$ [19].

To investigate the origin of the nematicity, FeSe ($T_c = 9$ K) is a favorable system since the electronic nematic state without magnetization is realized below $T_{\rm str} = 90$ K down to 0 K. Above $T_{\rm str}$, the antiferromagnetic fluctuation is weak and T independent according to the NMR [20,21] and neutron scattering [22–24] studies, in contrast to the sizable spin fluctuations above $T_{\rm str}$ in LaFeAsO [25] and $BaFe_2As_2$ [26]. This fact means that the magnetic instability is not a necessary condition for the electronic nematic state. In contrast to the smallness of the spin fluctuations, large nematic susceptibility is measured by C_{66} and $\Delta\rho$ in FeSe. Based on the orbital-spin fluctuation theory, called the self-consistent vertex-correction (SC-VC) theory, the development of the strong orbital fluctuations in FeSe are explained even when the spin-fluctuations are very small, consistent with experimental reports in FeSe [27]: The strong orbital fluctuations originate from the Aslamazov-Larkin vertex correction (AL-VC) that describes the orbital-spin mode-coupling [10]. The nematic charge density wave (CDW) in the cuprate superconductor also originates from the AL-VC [28,29].

The nontrivial electronic state below $T_{\rm str}$ gives a crucial test for the theories proposed so far. In the orthorhombic phase with $(a-b)/(a+b) \sim 0.3\%$, large orbital-splitting $|E_{xz} - E_{yz}|$ of order 50 meV is observed at X, Y points by angle-resolved photoemission spectroscopy (ARPES) studies in $BaFe_2As_2$ [30], NaFeAs [31], and FeSe [32–40]. Especially, noticeable deformation of the Fermi surfaces (FSs) with C_2 symmetry is realized in FeSe, because of the smallness of the Fermi momenta. In FeSe, Ref. [38] reports that the orbital splitting $E_{xz} - E_{yz}$ is positive at the Γ point, whereas it is negative at the X and Y points. This sign-reversing orbital splitting is not realized in the nonmagnetic orthorhombic phase in NaFeAs [31]. In addition, the electronlike FS1 (e-FS1) at the X point is deformed to two Dirac cone Fermi pockets in thin-film FeSe [37,40]. The aim of this Letter is to explain these nontrivial electronic states in the orbital-ordered states based on the realistic multiorbital Hubbard model.

Microscopically, the orbital order is expressed by the symmetry breaking in the self-energy. In the mean-field level approximations, however, the self-energy is constant in $\boldsymbol{k}$ space unless large intersite Coulomb interactions are introduced [13]. For this reason, we have to study the nonlocal correlation effect beyond the mean-field theory, based on the realistic Hubbard model with on-site Coulomb interaction. We will show that the strong positive feedback between the nematic orbital order and C_2-symmetric spin susceptibility plays the essential role.

In this Letter, we study the origin of the orbital order in Fe-based superconductors, by considering the cooperative symmetry breaking between the self-energy and spin susceptibility self-consistently. Experimentally observed strong $\boldsymbol{k}$-dependent orbital polarization $[\Delta E_{xz}(\boldsymbol{k}),$

$\Delta E_{yz}(\boldsymbol{k})]$ is given by the nonlocal self-energy with C_2 symmetry. In the FeSe model, we obtain the sign-reversing orbital-splitting $E_{xz} - E_{yz}$ between the Γ-point and the X and Y points reported in Refs. [38]. In addition, two Dirac-cone Fermi pockets emerge around the X point when the Coulomb interaction is larger [37,40]. Thus, important key experimental electronic properties in the orbital-ordered phase are satisfactorily explained.

Hereafter, we denote the five d-orbital $d_{3z^2-r^2}$, d_{xz}, d_{yz}, d_{xy}, $d_{x^2-y^2}$ as $l = 1, 2, 3, 4, 5$. We study the realistic eight-orbital d-p Hubbard models

$$H_M(r) = H_M^0 + rH_M^U (M = \text{LaFeAsO and FeSe}), \quad (1)$$

where H_M^U is the first-principles screened Coulomb potential for d orbitals in Ref. [41]: The averaged Coulomb interaction $\bar{U} \equiv \frac{1}{5}\sum_{l=1}^{5} U_l = 7.21$ eV for FeSe is much larger than $\bar{U} = 4.23$ eV for LaFeAsO, since the number of the screening bands, by which $\bar{U}$ is reduced, is small in FeSe [41]. In contrast, the averaged Hund's coupling $\bar{J} \equiv \frac{1}{10}\sum_{l>m} J_{l,m}$ is similar in all compounds since the screening on the Hund's coupling is small. For this reason, the ratio $\bar{J}/\bar{U} = 0.0945$ in FeSe is much smaller than the ratio $\bar{J}/\bar{U} = 0.134$ in LaFeAsO. The factor $r(<1)$ is introduced to adjust the spin fluctuation strength.

H_M^0 in Eq. (1) is the first-principle tight-binding model introduced in Ref. [27]. The band dispersion $E_{\boldsymbol{k}}^{\alpha}$ is the solution of $\det[\hat{z}^{-1}\epsilon + \mu - \hat{h}_M^0(\boldsymbol{k})] = 0$, where $\hat{h}_M^0(\boldsymbol{k})$ is the kinetic term and $\hat{z}^{-1}$ is the diagonal mass-enhancement factor: $(\hat{z}^{-1})_{l,l'} \equiv 1/z_l \delta_{l,l'}$. For LaFeAsO, we put $\hat{z}^{-1} = \hat{1}$. For FeSe, we put $1/z_4 = 1.6$ and $1/z_l = 1$ $(l \neq 4)$ to represent the strong renormalization of the d_{xy}-orbital band [32]. Figure 1 shows the band structures and the FSs in the FeSe and LaFeAsO models with $n_{\text{tot}} = 2\sum_{\alpha,\boldsymbol{k}} f(E_{\boldsymbol{k}}^{\alpha}) = 12$. In FeSe, each Fermi pocket is very shallow [42]. The detailed explanation for H_M^0 is given in the Supplemental Material (SM), Sec. A [43].

In this Letter, we calculate the $\boldsymbol{k}$ dependence of the self-energy using the self-consistent one-loop approximation, which has been applied to various single-orbital models [45] and multiorbital models [12] in literature. The Green function in the orbital basis is

$$\hat{G}(k) = [\hat{z}^{-1} i\epsilon_n + \mu - \hat{h}_M^0(\boldsymbol{k}) - \Delta\hat{\Sigma}(\boldsymbol{k})]^{-1}, \quad (2)$$

where $k = (\boldsymbol{k}, \epsilon_n = (2n+1)\pi T)$, $\Delta\hat{\Sigma}(\boldsymbol{k})$ is symmetry breaking self-energy. and $\hat{z}^{-1}$ is the diagonal mass-enhancement factor. The self-energy in the one-loop approximation [12,45] is given as

$$\Sigma_{l,l'}(k) = \Sigma_{l,l'}^H + T\sum_{q,m,m'} V_{l,m;l',m'}(q) G_{m,m'}(k-q), \quad (3)$$

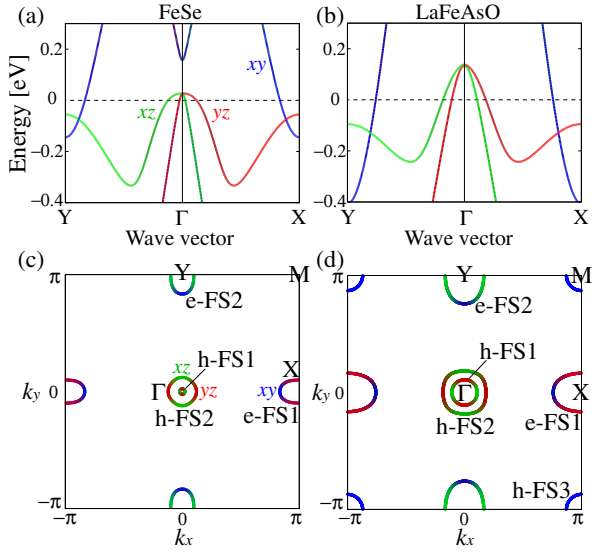

FIG. 1. Band structures of the eight-orbital models for (a) FeSe and (b) LaFeAsO in the unfolded Brillouin zone at $T = 50$ meV. FSs for the FeSe and LaFeAsO models are shown in (c) and (d), respectively. The colors correspond to 2 (green), 3 (red), and 4 (blue), respectively.

where $\Sigma_{l,l'}^H = -\sum_{m,m'} \Gamma_{l,l';m',m}^c \Delta n_{m,m'}$ is the Hartree term: $\Delta n_{m,m'} \equiv \langle c_{i,m,\sigma}^{\dagger} c_{i,m',\sigma}\rangle - \langle c_{i,m,\sigma}^{\dagger} c_{i,m',\sigma}\rangle_0$. The nonlocal interaction $\hat{V}(q)$ in Eq. (3) is given as $\frac{3}{2}\hat{\Gamma}^s\hat{\chi}^s(q)\hat{\Gamma}^s + \frac{1}{2}\hat{\Gamma}^c\hat{\chi}^c(q)\hat{\Gamma}^c - \frac{1}{2}[\hat{\Gamma}^c\hat{\chi}^0(q)\hat{\Gamma}^c + \hat{\Gamma}^s\hat{\chi}^0(q)\hat{\Gamma}^s - \frac{1}{4}(\hat{\Gamma}^s + \hat{\Gamma}^c)\hat{\chi}^0(q)(\hat{\Gamma}^s + \hat{\Gamma}^c)]$, where $\hat{\chi}^{s,c}(q) = \hat{\chi}^0(q)[1 - \hat{\Gamma}^{s,c}\hat{\chi}^0(q)]^{-1}$ and $\chi_{l,l',m,m'}^0(q) = -T\sum_k G_{l,m}(k+q) G_{m',l'}(k)$. Here, $\hat{\Gamma}^{c(s)}$ is the bare Coulomb interaction for the charge (spin) channel given in the SM, Sec. A [43].

From Eq. (3), the B_{1g}-type symmetry breaking self-energy included in Eq. (2), which is orbital diagonal, is derived as

$$\Delta\Sigma_l(\boldsymbol{k}) = \text{Re}\{\Sigma_{l,l}(\boldsymbol{k}, \epsilon_n) - \Sigma_l^{\text{A}_{1g}}(\boldsymbol{k}, \epsilon_n)\}_{i\epsilon_n \to 0}, \quad (4)$$

for $l = 2, 3$, where $\Sigma_l^{A_{1g}}(k) \equiv [\Sigma_{l,l}(k) + \Sigma_{5-l,5-l}(k')]/2$ $[\boldsymbol{k}' = (k_y, k_x)]$ is the A_{1g} component of the self-energy. In the present Letter, we calculate Eqs. (3) and (4) self-consistently [46]. We will show that $\Delta\Sigma_l$ emerges due to the strong positive feedback between the nematic orbital order and C_2-symmetric spin susceptibility: That is, near the nematic transition, infinitesimally small nematic orbital order enhances the spin susceptibility at $\boldsymbol{q} = (\pi, 0)$, and the enhanced spin-fluctuation-mediated interaction $\hat{V}(q)$, in turn, enlarges the orbital order.

First, we study the FeSe model, using 64×64 $\boldsymbol{k}$ meshes and 512 Matsubara frequencies at $T = 50$ meV. In FeSe, the orbital order with $\Delta E_{xz}(\boldsymbol{k}) \equiv \Delta\Sigma_2(\boldsymbol{k})$ and $\Delta E_{yz}(\boldsymbol{k}) \equiv \Delta\Sigma_3(\boldsymbol{k})$ emerges when the spin Stoner factor α_S, which is the maximum eigenvalue of $\hat{\Gamma}^s\hat{\chi}^0(\boldsymbol{q})$, is larger than 0.82 $(r > 0.253)$. The magnetic order is realized when $\alpha_S = 1$.

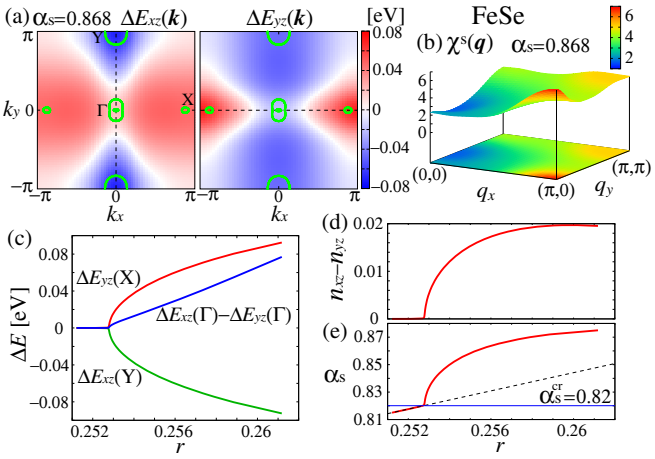

FIG. 2. (a) Orbital sign-reversing polarization $[\Delta E_{xz}(\boldsymbol{k}), \Delta E_{yz}(\boldsymbol{k})]$ and (b) $\chi^s(\boldsymbol{q})$ in the FeSe model for $\alpha_S = 0.868$ ($r = 0.257$). The realized FSs are shown by the green lines. The splitting $E_{xz} - E_{yz}$ at the Γ point is positive, as observed in Ref. [38]. (c) The polarization at Γ, X, and Y points. (d) $\Delta n \equiv n_{xz} - n_{yz}$, and (e) α_S for $0.261 > r > 0.251$.

In Figs. 2(a) and 2(b), we show, respectively, the obtained orbital polarization $[\Delta E_{xz}(\boldsymbol{k}), \Delta E_{yz}(\boldsymbol{k})]$, and the spin susceptibility $\chi^s(\boldsymbol{q}) \equiv \sum_{l,m} \chi^s_{l,l;m,m}(\boldsymbol{q})$ for $\alpha_S = 0.868$. Because of the positive $\Delta E_{yz}(X)$, the e-FS1 around the X point is modified to the pair of the Dirac-cone Fermi pockets. Another electron-pocket around the Y point, e-FS2, is enlarged by the negative $\Delta E_{xz}(Y)$. We stress that $\Delta E_{xz(yz)}(\boldsymbol{k})$ changes its sign along the $k_{y(x)}$ axis shown by the broken line in Fig. 2(a). Because of this sign reversal, the outer hole-pocket (h-FS2) is elongated along the k_y axis, as observed experimentally [38]. Because of the orbital polarization, α_S increases and $\chi^s(\boldsymbol{q})$ shows the C_2 anisotropy $\chi^s(\pi, 0) > \chi^s(0, \pi)$ shown in Fig. 2(b) [6,47].

In Fig. 2(c), we show the r dependences of the orbital polarization at the Γ, X, and Y points. With increasing r, the spin-fluctuation-driven orbital order appears as a second-order transition at $\alpha_S^{\rm cr} = 0.82$. The relations $\Delta E_{xz}(Y) < 0$ and $\Delta E_{yz}(X) > 0$ hold in the ordered state. In FeSe, the orbital splitting $E_{xz} - E_{yz}$ at the Γ point is positive, so h-FS2 is elongated along the k_y axis. Such sign-reversing orbital order does not occur in the LaFeAsO model (see Fig. 5). Since d_{xz} and d_{yz} orbitals are exchanged by $\pi/2$ rotation, the obtained order $[\Delta E_{xz}(\boldsymbol{k}), \Delta E_{yz}(\boldsymbol{k})]$ belongs to the B_{1g} representation (=d wave), in spite of $\Delta E_{xz}(\boldsymbol{k}) \neq \Delta E_{yz}(\boldsymbol{k})$ [13,36].

Figure 2(d) shows the difference $\Delta n \equiv n_{xz} - n_{yz}$: $\Delta n \sim +10^{-2}$ will induce the small lattice deformation $(a-b)/(a+b) \approx 0.2\%$ in FeSe due to small e-ph interaction. When $\Delta n \neq 0$, the spin Stoner factor α_S is strongly enlarged as shown in Fig. 2(e), consistent with the enhancement of spin fluctuations observed by NMR [20,21] and neutron [22,23] measurements. For a fixed r, Δn shows a mean-field-type second-order T dependence below $T_{\rm str}$ [27].

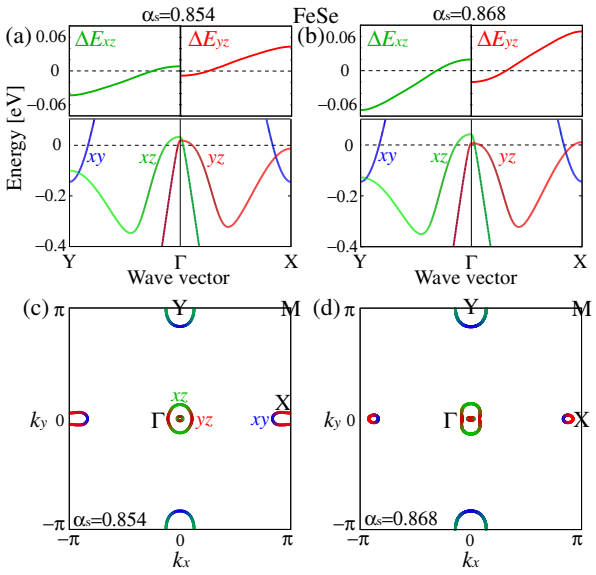

FIG. 3. Orbital polarizations and band structures in the FeSe model along $Y \to \Gamma \to X$ for (a) $\alpha_S = 0.854$ and (b) $\alpha_S = 0.868$. The corresponding FSs at $T = 50$ meV are shown in (c) and (d), respectively.

In Fig. 3, we display the C_2 band structures obtained in the FeSe model for (a) $\alpha_S = 0.854$ and (b) $\alpha_S = 0.868$. In both cases, $\Delta E_{yz}(k_x, 0)$ and $\Delta E_{xz}(0, k_y)$ show sign reversal, and $E_{xz} - E_{yz} > 0$ at the Γ point. The shape of the FSs in Fig. 3(c) for $\alpha_S = 0.854$ (Fig. 3(d) for $\alpha_S = 0.868$) is consistent with the FSs observed in bulk FeSe (thin-film FeSe). This result indicates that the electron correlation in thin-film FeSe is slightly stronger, consistent with the higher $T_{\rm str} \approx 120$ K in thin-film FeSe.

In real FeSe, the inner pocket sinks under the Fermi level due to the spin-orbit interaction. A similar single hole FS model is introduced in the SM, Sec. B [43] by shifting the d_{xy} orbital level at the Γ point. It is verified that the sign-reversing orbital polarization emerges in the FeSe model with single hole FS in the SM, Sec. B [43].

Here, we explain that the origin of the orbital order is the positive feedback between the orbital polarization $[\Delta E_{xz}(\boldsymbol{k}), \Delta E_{yz}(\boldsymbol{k})]$ and the spin susceptibility. For this purpose, we introduce the following two simplified self-energies and perform the self-consistent calculations:

$$\Sigma^{\rm AL}_{l,l'}(k) = \Sigma^{H}_{l,l'} + T \sum_{q,m,m'} V_{l,m;l',m'}(q) G^{\Delta E=0}_{m,m'}(k-q), \quad (5)$$

$$\Sigma^{\rm MT}_{l,l'}(k) = \Sigma^{H}_{l,l'} + T \sum_{q,m,m'} V^{\Delta E=0}_{l,m;l',m'}(q) G_{m,m'}(k-q), \quad (6)$$

where the superscript "$\Delta E = 0$" means the absence of the C_2 orbital polarization. In Eq. (5) [Eq. (6)], only the feedback effect from the symmetry-breaking spin susceptibility (Green function) is included. $\hat{\Sigma}^{\rm AL(MT)}$ contains the Aslamazov-Larkin term (Maki-Thompson (MT) term) that is the second-order (first-order) term with respect to

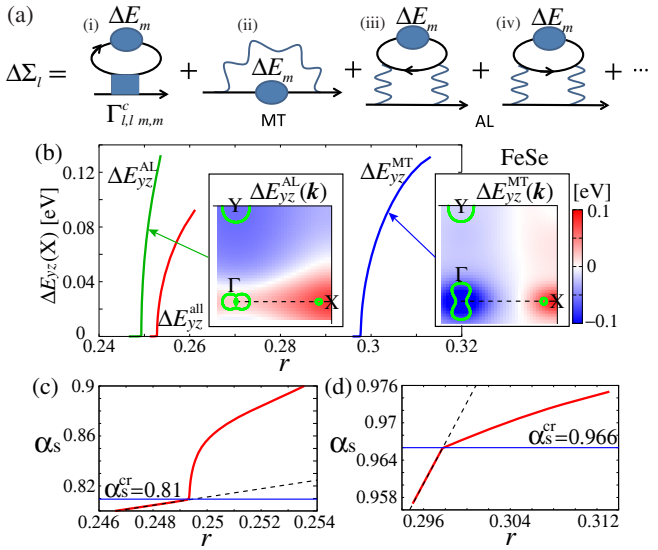

FIG. 4. (a) Expansion of the self-energy with respect to ΔE. The MT term (AL term) is included in $\hat{\Sigma}^{\mathrm{MT(AL)}}$. (b) r dependences of $\Delta E_{yz}^{\mathrm{AL}}$ and $\Delta E_{yz}^{\mathrm{MT}}$ at the X point. $\Delta E_{yz}^{\mathrm{all}}$ is the orbital polarization derived from Eq. (3) shown in Fig. 2 (c). (c) α_S due to $\hat{\Sigma}^{\mathrm{AL}}$, and (d) α_S due to $\hat{\Sigma}^{\mathrm{MT}}$.

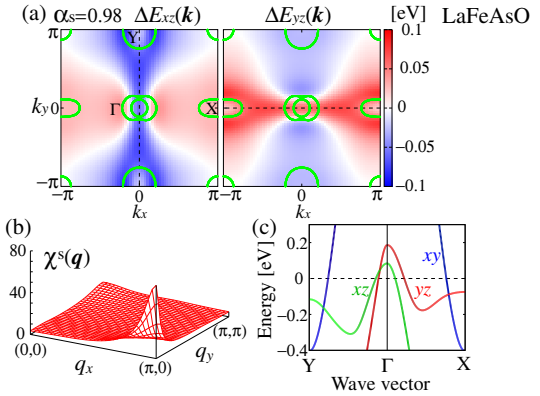

FIG. 5. (a) Obtained sign-preserving orbital polarization $[\Delta E_{xz}(\boldsymbol{k}), \Delta E_{yz}(\boldsymbol{k})]$ in the LaFeAsO model for $\alpha_S = 0.98$ ($r = 0.376$). The FSs are shown by the green lines. The corresponding spin susceptibility and the band structure are shown in (b) and (c), respectively.

χ^s in Fig. 4(a), which shows the expansion of the self-energy in Eq. (3) by using the relation $\hat{G} = \hat{G}^{\Delta E=0} + \hat{G}^{\Delta E=0}\Delta\hat{E}\hat{G}^{\Delta E=0} + O(\Delta E^2)$; see the SM, Sec. C [43] for detailed explanation. Figure 4(b) shows the orbital polarizations $\Delta E_{yz}^{\mathrm{AL}}$ and $\Delta E_{yz}^{\mathrm{MT}}$ at the X point derived from Eqs. (5) and (6), respectively, as functions of r at $T = 50$ meV. Here, $\Delta E_{yz}^{\mathrm{all}}$ is the orbital polarization derived from Eq. (3), shown in Fig. 2(c). The closeness of $\Delta E_{yz}^{\mathrm{AL}}$ and $\Delta E_{yz}^{\mathrm{all}}$ means that the orbital order is mainly driven by the Aslamazov-Larkin term $\hat{\Sigma}^{\mathrm{AL}}$. Figure 4(c) shows that α_S is strongly enlarged by the orbital order due to $\hat{\Sigma}^{\mathrm{AL}}$, similar to α_S in Fig. 2(e). In contrast, α_S in Fig. 4(d) is suppressed because of the wrong $\boldsymbol{q} = (\pi, 0)$ nesting on the d_{yz} orbital due to $\hat{\Sigma}^{\mathrm{MT}}$. Thus, the origin of the orbital order is the strong positive feedback between the orbital polarization and C_2 spin susceptibility described by the Aslamazov-Larkin term in Eq. (5).

Although $\hat{\Sigma}^{\mathrm{AL}}$ is the main driving force of the orbital order, the hole pocket is elongated along the k_x axis in the ordered state driven by $\hat{\Sigma}^{\mathrm{AL}}$ as shown in the left inset of Fig. 4(b). Therefore, the Maki-Thompson term is indispensable for reproducing the sign-reversing orbital polarization; see the right inset of Fig. 4(b). In the SM, Sec. C [43], we analytically explain why the Maki-Thompson term gives the sign reversal. Thus, although $\Delta E_{yz}^{\mathrm{AL}}(k_x, 0)$ is always positive as shown in the left inset of Fig. 4(b), $\Delta E_{yz}^{\mathrm{all}}(k_x, 0)$ in Fig. 2(a) given by Eq. (3) changes to negative at $k_x \sim 0$, due to the sign-reversing Maki-Thompson term that is small in magnitude at $\alpha_S \gtrsim \alpha_S^{\mathrm{cr}}$.

Next, we show the numerical results for the LaFeAsO model with $\hat{z}^{-1} = \hat{1}$. Then, the orbital order is realized for $\alpha_S > 0.91$. In Fig. 5(a), we show the obtained orbital polarization at $\alpha_S = 0.98$ and $T = 47$ meV. The e-FS1 around the X point is smaller than e-FS2 around the Y point due to the orbital polarization $\Delta E_{xz}(Y) < 0$ and $\Delta E_{yz}(X) > 0$. In addition, $\Delta E_{yz}(k_x, 0)$ ($\Delta E_{xz}(0, k_y)$) is always positive (negative), and therefore, the outer hole pocket is elongated along the k_x axis. This result is consistent with the Fermi surface deformation in the nonmagnetic orthorhombic phase in NaFeAs [31]. In the ordered state, strong in-plane anisotropy of the spin susceptibility $\chi^s(\pi, 0) \gg \chi^s(0, \pi)$ is realized as shown in Fig. 5(b) [47], consistent with the neutron scattering experiments. The band structure is shown in Fig. 5(c).

In this Letter, we succeeded in explaining (i) the small critical Stoner factor α_S^{cr} and (ii) the relation $E_{xz} > E_{yz}$ near the Γ point in FeSe. An origin of (i) is the smallness of the ratio $\bar{J}/\bar{U}$, as verified by the SC-VC theory [27] and the renormalization group (RG) theory [48,49]. Another origin of (i) is the smallness of the FSs in FeSe, since the three-point vertex $\hat{\Lambda}_3 \equiv \delta\hat{\chi}^0(\boldsymbol{q})/\delta\Delta\hat{E}$ in the Aslamazov-Larkin term increases when the particle-hole asymmetry is large [27]. The relation (ii) can be realized by the sign-reversing Maki-Thomson term. Although the Maki-Thompson term is usually small, (ii) is actually realized when the FSs are smaller since the minimum of the Aslamazov-Larkin term $\Delta E_{yz}^{\mathrm{AL}}(\boldsymbol{k})$ shifts to $\boldsymbol{k} = \boldsymbol{0}$. Recently, the advantage of the small FSs for the nematicity has been stressed by the RG study in Ref. [50].

In summary, we investigated the C_2 symmetry breaking in the self-energy and susceptibility self-consistently, and explained the experimental C_2-symmetric FSs and $\chi^s(\boldsymbol{q})$. In the FeSe model, experimental deformation of the FSs due to the sign-reversing orbital polarization is satisfactorily reproduced. In the LaFeAsO model, in contrast, spin

fluctuations are strongly enlarged by the sign-preserving orbital polarization. Thus, the key experiments below T_{str} are satisfactorily explained. The orbital order originates from the positive feedback between the nematic orbital order and spin susceptibility due to the Aslamazov-Larkin term, and the sign reversal of $\Delta E_{yz}(k_x, 0)$ and $\Delta E_{xz}(0, k_y)$ in FeSe is caused by the Maki-Thompson term.

We are grateful to Y. Matsuda, T. Shibauchi, T. Shimojima, A. Chubukov, J. Schmalian, and R. Fernandes for useful discussions. This Letter was supported by JSPS KAKENHI Grants No. JP26800185 and No. JP15H03687. Part of numerical computation in this Letter was carried out at the Yukawa Institute Computer Facility.

[1] R. M. Fernandes, L. H. VanBebber, S. Bhattacharya, P. Chandra, V. Keppens, D. Mandrus, M. A. McGuire, B. C. Sales, A. S. Sefat, and J. Schmalian, Phys. Rev. Lett. **105**, 157003 (2010).
[2] F. Wang, S. A. Kivelson, and D.-H. Lee, Nat. Phys. **11**, 959 (2015).
[3] A. V. Chubukov, R. M. Fernandes, and J. Schmalian, Phys. Rev. B **91**, 201105 (2015).
[4] R. Yu and Q. Si, Phys. Rev. Lett. **115**, 116401 (2015).
[5] J. K. Glasbrenner, I. I. Mazin, H. O. Jeschke, P. J. Hirschfeld, and R. Valenti, Nat. Phys. **11**, 953 (2015).
[6] L. Fanfarillo, A. Cortijo, and B. Valenzuela, Phys. Rev. B **91**, 214515 (2015).
[7] F. Krüger, S. Kumar, J. Zaanen, and J. van den Brink, Phys. Rev. B **79**, 054504 (2009).
[8] W. Lv, J. Wu, and P. Phillips, Phys. Rev. B **80**, 224506 (2009).
[9] C.-C. Lee, W.-G. Yin, and W. Ku, Phys. Rev. Lett. **103**, 267001 (2009).
[10] S. Onari and H. Kontani, Phys. Rev. Lett. **109**, 137001 (2012).
[11] S. Onari, Y. Yamakawa, and H. Kontani, Phys. Rev. Lett. **112**, 187001 (2014).
[12] S. Onari and H. Kontani, in *Iron-Based Superconductivity*, edited by P. D. Johnson, G. Xu, and W.-G. Yin (Springer-Verlag Berlin, 2015).
[13] K. Jiang, J. P. Hu, H. Ding, and Z. Wang, Phys. Rev. B **93**, 115138 (2016).
[14] M. Yoshizawa, D. Kimura, T. Chiba, S. Simayi, Y. Nakanishi, K. Kihou, C.-H. Lee, A. Iyo, H. Eisaki, M. Nakajima, and S. Uchida, J. Phys. Soc. Jpn. **81**, 024604 (2012).
[15] A. E. Böhmer, P. Burger, F. Hardy, T. Wolf, P. Schweiss, R. Fromknecht, M. Reinecker, W. Schranz, and C. Meingast, Phys. Rev. Lett. **112**, 047001 (2014).
[16] Y. Gallais, R. M. Fernandes, I. Paul, L. Chauviere, Y.-X. Yang, M.-A. Measson, M. Cazayous, A. Sacuto, D. Colson, and A. Forget, Phys. Rev. Lett. **111**, 267001 (2013).
[17] H. Kontani and Y. Yamakawa, Phys. Rev. Lett. **113**, 047001 (2014).
[18] M. Khodas and A. Levchenko, Phys. Rev. B **91**, 235119 (2015).
[19] J.-H. Chu, H.-H. Kuo, J. G. Analytis, and I. R. Fisher, Science **337**, 710 (2012).
[20] A. E. Böhmer, T. Arai, F. Hardy, T. Hattori, T. Iye, T. Wolf, H. v. Löhneysen, K. Ishida, and C. Meingast, Phys. Rev. Lett. **114**, 027001 (2015).
[21] S.-H. Baek, D. V. Efremov, J. M. Ok, J. S. Kim, J. van den Brink, and B. Büchner, Nat. Mater. **14**, 210 (2015).
[22] M. C. Rahn, R. A. Ewings, S. J. Sedlmaier, S. J. Clarke, and A. T. Boothroyd, Phys. Rev. B **91**, 180501(R) (2015).
[23] Q. Wang, Y. Shen, B. Pan, Y. Hao, M. Ma, F. Zhou, P. Steffens, K. Schmalzl, T. R. Forrest, M. Abdel-Hafiez, D. A. Chareev, A. N. Vasiliev, P. Bourges, Y. Sidis, H. Cao, and J. Zhao, Nat. Mater. **15**, 159 (2016).
[24] S. Shamoto, K. Matsuoka, R. Kajimoto, M. Ishikado, Y. Yamakawa, T. Watashige, S. Kasahara, M. Nakamura, H. Kontani, T. Shibauchi, and Y. Matsuda, arXiv:1511.04267.
[25] Y. Nakai, S. Kitagawa, T. Iye, K. Ishida, Y. Kamihara, M. Hirano, and H. Hosono, Phys. Rev. B **85**, 134408 (2012).
[26] F. L. Ning, K. Ahilan, T. Imai, A. S. Sefat, M. A. McGuire, B. C. Sales, D. Mandrus, P. Cheng, B. Shen, and H.-H Wen, Phys. Rev. Lett. **104**, 037001 (2010).
[27] Y. Yamakawa, S. Onari, and H. Kontani, arXiv:1509.01161 [Phys. Rev. X (to be published)].
[28] Y. Yamakawa and H. Kontani, Phys. Rev. Lett. **114**, 257001 (2015).
[29] M. Tsuchiizu, Y. Yamakawa, and H. Kontani, Phys. Rev. B **93**, 155148 (2016).
[30] M. Yi, D. Lu, J.-H. Chu, J. G. Analytis, A. P. Sorini, A. F. Kemper, B. Moritz, S.-K. Mo, R. G. Moore, M. Hashimoto, W.-S. Lee, Z. Hussain, T. P. Devereaux, I. R. Fisher, and Z.-X. Shen, Proc. Natl. Acad. Sci. U.S.A. **108**, 6878 (2011).
[31] Y. Zhang, C. He, Z. R. Ye, J. Jiang, F. Chen, M. Xu, Q. Q. Ge, B. P. Xie, J. Wei, M. Aeschlimann, X. Y. Cui, M. Shi, J. P. Hu, and D. L. Feng, Phys. Rev. B **85**, 085121 (2012).
[32] J. Maletz, V. B. Zabolotnyy, D. V. Evtushinsky, S. Thirupathaiah, A. U. B. Wolter, L. Harnagea, A. N. Yaresko, A. N. Vasiliev, D. A. Chareev, A. E. Böhmer, F. Hardy, T. Wolf, C. Meingast, E. D. L. Rienks, B. Büchner, and S. V. Borisenko, Phys. Rev. B **89**, 220506(R) (2014).
[33] K. Nakayama, Y. Miyata, G. N. Phan, T. Sato, Y. Tanabe, T. Urata, K. Tanigaki, and T. Takahashi, Phys. Rev. Lett. **113**, 237001 (2014).
[34] M. D. Watson, T. K. Kim, A. A. Haghighirad, N. R. Davies, A. McCollam, A. Narayanan, S. F. Blake, Y. L. Chen, S. Ghannadzadeh, A. J. Schofield, M. Hoesch, C. Meingast, T. Wolf, and A. I. Coldea, Phys. Rev. B **91**, 155106 (2015).
[35] T. Shimojima, Y. Suzuki, T. Sonobe, A. Nakamura, M. Sakano, J. Omachi, K. Yoshioka, M. Kuwata-Gonokami, K. Ono, H. Kumigashira, A. E. Böhmer, F. Hardy, T. Wolf, C. Meingast, H. v. Löhneysen, H. Ikeda, and K. Ishizaka, Phys. Rev. B **90**, 121111(R) (2014).
[36] P. Zhang, T. Qian, P. Richard, X. P. Wang, H. Miao, B. Q. Lv, B. B. Fu, T. Wolf, C. Meingast, X. X. Wu, Z. Q. Wang, J. P. Hu, and H. Ding, Phys. Rev. B **91**, 214503 (2015).
[37] Y. Zhang, M. Yi, Z.-K. Liu, W. Li, J. J. Lee, R. G. Moore, M. Hashimoto, N. Masamichi, H. Eisaki, S.-K. Mo, Z. Hussain, T. P. Devereaux, Z.-X. Shen, and D. H. Lu, arXiv:1503.01556.
[38] Y. Suzuki, T. Shimojima, T. Sonobe, A. Nakamura, M. Sakano, H. Tsuji, J. Omachi, K. Yoshioka, M. Kuwata-Gonokami, T. Watashige, R. Kobayashi, S. Kasahara,

T. Shibauchi, Y. Matsuda, Y. Yamakawa, H. Kontani, and K. Ishizaka, Phys. Rev. B **92**, 205117 (2015).
[39] M. D. Watson, T. K. Kim, A. A. Haghighirad, S. F. Blake, N. R. Davies, M. Hoesch, T. Wolf, and A. I. Coldea, Phys. Rev. B **92**, 121108 (2015).
[40] S. Y. Tan, Y. Fang, D. H. Xie, W. Feng, C. H. P. Wen, Q. Song, Q. Y. Chen, W. Zhang, Y. Zhang, L. Z. Luo, B. P. Xie, X. C. Lai, and D. L. Feng, Phys. Rev. B **93**, 104513 (2016).
[41] T. Miyake, K. Nakamura, R. Arita, and M. Imada, J. Phys. Soc. Jpn. **79**, 044705 (2010).
[42] S. Kasahara, T. Watashige, T. Hanaguri, Y. Kohsaka, T. Yamashita, Y. Shimoyama, Y. Mizukami, R. Endo, H. Ikeda, K. Aoyama, T. Terashima, S. Uji, T. Wolf, H. v. Löhneysen, T. Shibauchi, and Y. Matsuda, Proc. Natl. Acad. Sci. U.S.A. **111**, 16309 (2014).
[43] See Supplemental Material at http://link.aps.org/supplemental/10.1103/PhysRevLett.116.227001 for the orbital order at $T = 25$ meV, the orbital order in the single-hole-pocket model, and the relationship between the present C_2 self-energy study for $T < T_{\rm str}$ and the SC-VC theory for $T > T_{\rm str}$, which includes Ref. [44].
[44] T. Saito, Y. Yamakawa, S. Onari, and H. Kontani, Phys. Rev. B **92**, 134522 (2015).
[45] N. E. Bickers and S. R. White, Phys. Rev. B **43**, 8044 (1991).
[46] We verified that the critical value of r for the orbital order is slightly enlarged if Eq. (4) is replaced with $\Delta\Sigma_l(\boldsymbol{k}, \epsilon_n) = \{\Sigma_{l,l}(k, \epsilon_n) - \Sigma_l^{\rm A_{1g}}(\boldsymbol{k}, \epsilon_n)\}$.
[47] H. Kontani, T. Saito, and S. Onari, Phys. Rev. B **84**, 024528 (2011).
[48] M. Tsuchiizu, Y. Ohno, S. Onari, and H. Kontani, Phys. Rev. Lett. **111**, 057003 (2013).
[49] M. Tsuchiizu, Y. Yamakawa, S. Onari, Y. Ohno, and H. Kontani, Phys. Rev. B **91**, 155103 (2015).
[50] A. V. Chubukov, M. Khodas, and R. M. Fernandes, arXiv:1602.05503.